The Space and Scale Dependencies of the Self-Similar Structure of Turbulence
Author(s): N. K.-R. Kevlahan and J. C. Vassilicos
Source: *Proceedings: Mathematical and Physical Sciences*, Vol. 447, No. 1930 (Nov. 8, 1994), pp. 341-363
Published by: The Royal Society
Stable URL: http://www.jstor.org/stable/52620
Accessed: 16/10/2009 11:51

The space and scale dependencies of the self-similar structure of turbulence

BY N. K.-R. KEVLAHAN AND J. C. VASSILICOS

Department of Applied Mathematics and Theoretical Physics, University of Cambridge, Silver Street, Cambridge CB3 9EW, U.K.

Two new techniques for analysing the space and scale dependencies of the self-similar structure of turbulence are introduced. Both methods are based on the wavelet transform, but use different wavelets.

First, the concept of a 'turbulence eddy' is defined in terms of the Mexican hat wavelet transform of the velocity signal in such a way that the 'eddy' has a size and a location in space. A new scaling exponent, the eddy capacity D_{E} ($0 \leqslant D_{\mathrm{E}} \leqslant 1$), is defined in terms of the zero crossings of this wavelet transform. D_{E} is a measure of the space-fillingness of eddies and of their scaling in *real space* whereas the Hausdorff dimension D'_{H} and the Kolmogorov capacity D'_{K} are scaling exponents that are sensitive to the scaling and space-fillingness in wavenumber space. D_{E} differs from both D'_{K} and D'_{H} in that it is particularly sensitive to phase correlations. For any random phase signal, $D_{\mathrm{E}} = 1$, whereas D'_{H} and D'_{K} depend on the energy spectrum. For well defined spiral signals, and for signals with a fractal intermittency in space, $D_{\mathrm{E}} = D'_{\mathrm{K}}$.

Secondly, we propose a practical test for discriminating between H-fractals and K-fractals (i.e. between a dense and a sparse distribution of singularities). This method is based on successive averages of wavelet transforms, and the Morlet wavelet is used. The technique is shown to be robust with respect to large amounts of phase noise.

Both methods are applied to a one-dimensional (1D) turbulence velocity signal of very high Reynolds number $Re_\lambda = 2720$. It is found that $D_{\mathrm{E}} = 1$ for the inertial scales larger than the Taylor microscale λ, thus indicating some degree of phase scrambling of the 1D turbulence velocity signal at the larger inertial scales. There is some indication of a spiral-type structure in this signal at scales below λ.

Finally, we measure the spatial fluctuation of wavelet energy, comparing an experimental turbulence signal with random phase and spiral-like signals. The magnitude of spatial fluctuations is set by the scrambled phase part of the turbulence, but the increase of energy fluctuation at small scales may be due to locally self-similar small-scale structures.

1. Introduction

Recent direct numerical simulations (DNS) suggest that turbulence consists of small scale coherent flow structures evolving in and interacting with the surrounding larger scale and approximately gaussian 'sea' (Jiménez *et al.* 1993 and references therein). The gradual departure from gaussianity at the finer scales of

Proc. R. Soc. Lond. A (1994) **447**, 341–363
Printed in Great Britain

turbulent motion has also been detected in high Reynolds number experiments, both recently (Gagne *et al.* 1988) and more than 40 years ago (Batchelor 1953).

Although DNS data do not always reproduce unequivocally Kolmogorov's celebrated $-\frac{5}{3}$ law because of current limitations in resolution and Reynolds number, experimental data do exhibit a well defined self-similar inertial range when the Reynolds number is very large (Gagne *et al.* 1988). The exponent $2p$ that characterizes the scaling of the energy spectrum $E(k) \sim k^{-2p}$ is close to $\frac{5}{3}$, and is defined over a wide range of length scales. In the experiments of Gagne *et al.* (1988), the self-similar inertial scales range from order of tens of metres to centimetres. The degree of non-gaussianity of 'eddies' (here referring only to wavenumbers) varies over this range of scales, yet the scaling of the energy spectrum remains the same. Kolmogorov's $-\frac{5}{3}$ law extends from relatively large inertial scales where the turbulence appears to have the form of a large scale gaussian background to smaller scales where the turbulence is structured and takes the form of vortex tubes (see, for example, Jiménez *et al.* 1993).

Hunt & Vassilicos (1991) have shown that there must be singularities in the turbulence field associated with a non-integer power p of the energy spectrum's scaling. These singularities can be of a power law type such as the $1/r$ dependence of the velocity around a two-dimensional (2D) point vortex (where r is the distance to the centre of the vortex in the 2D plane), a spiral type local accumulation of length scales (e.g. spiral vortex sheets), or a fractal type global accumulation of length scales (e.g. fractional brownian motions).

Turbulence has some similarities with fractional brownian motions at the large scale end of the inertial range, but in the small scale part of the inertial range the vorticity is concentrated into tubes. The internal structure of these tubes is still unknown; they could be the result of incidental superpositions of high strain with high vorticity, or of some kind of shear instability that transforms strain generated vortex sheets into spiral vortex tubes. In either case, these tubes will contribute to the scaling of the energy spectrum, but only at the smaller inertial length scales. Vassilicos & Hunt (1991) and Hunt & Vassilicos (1991) make the point that the self-similarity of the energy spectrum may reflect either of two types of self-similar structure in the topology of the velocity or vorticity fields: a locally self-similar structure and a globally self-similar structure. Examples of the first type of self-similarity include fields such as the spiral of a rolled-up vortex sheet which are self-similar only about a finite number of isolated points, while fields which are globally self-similar (e.g. fractional brownian motion) are self-similar about every point. A non-integer Kolmogorov capacity D_{K} (also referred to as 'fractal' or box dimension)† characterizes both these self-similar structure types, but D_{K} alone cannot discriminate between local and global self-similarity.

Either type of self-similarity may be present in the turbulence, at different scales and at different locations. The gradual departure from gaussianity over increasingly small scales of motion suggests a self-similar structure of the turbulence that is global at the larger inertial scales but may be local at the smaller inertial scales if, for example, the vortex tubes prove to have a complex internal structure that is locally self-similar (e.g. a spiral vortex). It has been proved mathematically

† D'_{K} and D'_{H} are, respectively, the Kolmogorov capacity and Hausdorff dimension of the set of points on the 1D cross-section through a graph, line or surface of capacity D_{K} and Hausdorff dimension D_{H}.

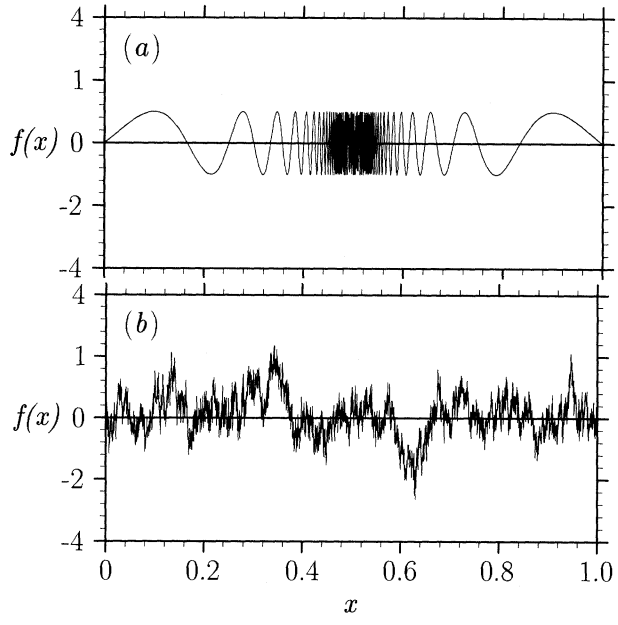

Figure 1. (*a*) $\sin(2\pi/x)$ spiral. (*b*) Scrambled phase version of (*a*).

that fractional brownian motions, or gaussian velocity fields, are characterized by non-integer Kolmogorov capacities D_{K} and non-integer Hausdorff dimensions D_{H} (see references in Mandelbrot (1982)). It is also mathematically well established that certain spirals have non-integer Kolmogorov capacities D_{K}, although their Hausdorff dimension is trivial (Mendès-France 1991).

Vassilicos & Hunt (1991) distinguish between local and global self-similarity as follows: if D_{H} is an integer and $D_{\mathrm{H}} < D_{\mathrm{K}}$ then the self-similarity is local and the object is called K-fractal; if D_{H} is non-integer the self-similarity is global and the object is called H-fractal. Unfortunately Hausdorff dimensions cannot be measured in practise (D_{H} can only be estimated by measuring D_{K} if the signal is truly H-fractal). It is therefore important to discover *practical* criteria that can be used to discriminate between local and global self-similarity.

In § 3 we propose such a criterion based on successive averages of the wavelet transform of a signal. It turns out that averaging is not always equivalent to phase scrambling (physical location information is not always lost after averaging). The nature of the phase correlations is intimately related to the global or local nature of the self-similar multiple scale structure of a signal (as pointed out by Hunt *et al.* 1993). Scrambling the phases of a signal's Fourier transform and then transforming back to physical space will convert a locally self-similar signal into a globally self-similar one with the same energy spectrum (see figure 1).

The difference between local and global self-similarity is essentially a difference between sparse and dense sets of singularities, and surprisingly, the wavelet transform can exploit this number theoretical difference in practical ways. The behaviour of successive averages of the wavelet transform of a self-similar signal can be used to determine whether the set of singularities in the signal are sparse or dense, and therefore whether the various scales have a fractal or a 'spiral' structure. In § 3 this test is applied to the very high Reynolds number experimental

turbulence data of Gagne *et al.* (1988). This is done in the hope of determining the nature of the self-similarity at the small inertial scales of turbulence where the dynamics are dominated by the vortex tubes.

In § 2 the larger inertial scales of turbulence are investigated using a novel method based on the wavelet transform. This method re-defines the now well-established, but imprecise, *statistical* concept of an 'eddy'. Statistical eddies in turbulence are defined classically in terms of Fourier transforms and do not have a location in physical space (Batchelor 1953). We use the zero-crossings of the Mexican Hat wavelet transform to define eddies having spatial location and introduce a new 'eddy capacity' (or dimension) D_{E}. The space fillingness of the experimental turbulence data is characterized by measuring D_{E}. This new definition of an 'eddy' allows us to reinterpret and characterize the classical Richardson cascade on the basis of modern concepts such as D_{E} and the wavelet transformed turbulence. In particular, a direct definition of the space-fillingness, or intermittency, of the eddies in the Richardson cascade is now possible. This space-scale characterization of turbulence was not feasible using the traditional interpretation of an eddy in terms of sine waves. Our concept of space-fillingness is new and distinct from previous concepts of space-fillingness that are based on either the Kolmogorov capacity or the Hausdorff dimension. Unlike D_{K} and D_{H}, the eddy capacity D_{E} reaches its maximal value, indicating complete space-fillingness, only when the Fourier phases are uncorrelated, regardless of the power spectrum's scaling.

It should be noted here that the concept of an 'eddy' is used in a statistical sense in our study of the larger inertial scales, but in a deterministic sense (in terms of the actual position of vortex tubes) in our study of the smaller inertial scales of the turbulence. The definition of an 'eddy' of a given scale depends on how far from gaussian the turbulence is at that scale.

In § 4 the spatial fluctuation of wavelet energy is measured as a function of scale for experimental turbulence data and compared to sample spiral-like and random phase self-similar signals with the same energy spectrum ($E(k) \propto k^{-5/3}$). The aim is to understand which aspects of energy fluctuations can be accounted for by the scrambled phase part of the inertial range turbulence, and which aspects require the presence of local small-scale coherent structures.

2. Is the Richardson cascade space-filling?

Richardson (1922) imagined turbulence as a hierarchy of eddies from large to small with the smaller eddies 'feeding' on the larger ones until the energy eventually passes into heat through viscosity at the smallest scales of motion. This metaphor has been found to give a good picture of energy dynamics in the inertial range of turbulence, but the precise nature of the 'eddies' remains unclear. Are these eddies 'space filling' in some sense (e.g. twice as many eddies of scale a as eddies of scale $2a$)? Are they physically separate structures? What is their distribution in space? To address these questions we need a new definition of a statistical 'eddy' that involves both scale and location. Fourier methods concentrate on the periodicities in the signal and do not provide a practical way to *locate* these periodicities in real space. The wavelet transform, however, is a new

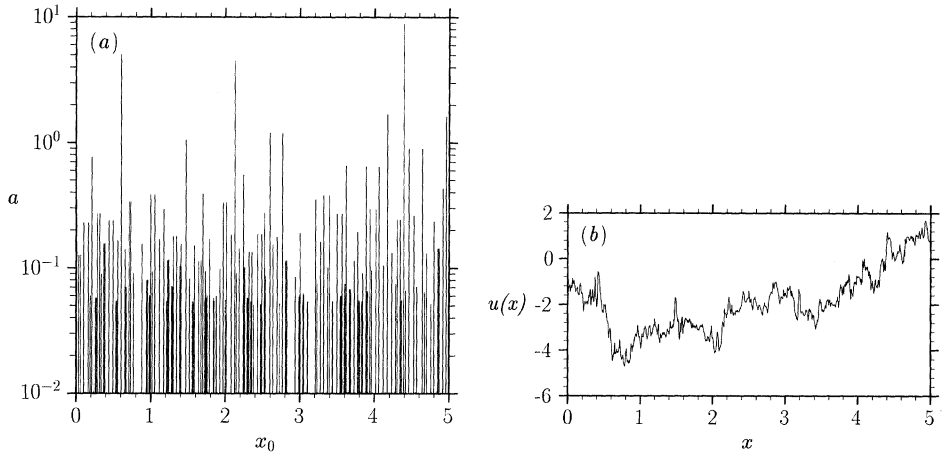

Figure 2. (*a*) Straightened zero crossings of the Mexican hat wavelet transform of a 1200 point long segment of the longitudinal component of an experimental turbulent velocity signal. (*b*) Original signal.

mathematical tool which enables the simultaneous study of both the periodicities in the signal and the physical location of these periodicities along the signal.

We define a turbulence eddy, in terms of Vermeer & Alkemade's (1993) method of multiscale segmentation of well logs. These authors use the zero-crossings of a specific wavelet transform to detect edges or drops in a signal. The wavelet transform $\tilde{u}(x_0, a)$ of a one-dimensional turbulence velocity signal $u(x)$ is, by definition,

$$\tilde{u}(x_0, a) = a^{-1/2} \int_{-\infty}^{+\infty} u(x) \psi^* \left(\frac{x - x_0}{a} \right) \mathrm{d}x, \tag{2.1}$$

where a is the length scale, x_0 is the location and the function $\psi(x)$ is the 'mother' wavelet (see Farge *et al.* 1993). Following Vermeer & Alkemade (1993), we choose a Mexican hat wavelet, that is $\psi(x) = \mathrm{d}^2/\mathrm{d}x^2 \exp(-\frac{1}{2}x^2)$. Provided that $u(x)$ is twice differentiable, this wavelet transform maps the second derivative of $u(x)$ at asymptotically small scales a. Zeros of $\tilde{u}(x_0, a)$ tend towards zeros of $\mathrm{d}^2/\mathrm{d}x^2 u(x_0)$ as $a \to 0$.

In figure 2*a* we plot the 'straightened zero-crossings' of the Mexican hat wavelet transform of a high Reynolds number experimental turbulence velocity signal $u(x)$, and in figure 2*b* we plot $u(x)$. The zero-crossings of the wavelet transform are long curves in the (x_0, a) plane that point towards a location on the x_0 axis. The 'straightened zero crossing' lines are found by determining the maximum length scale and position $(a_{\max}, x_0)$ at which a zero crossing appears and connecting this point to the $x-$axis by a straight line. Visibly, the longer curves point towards an x_0 where there is a sudden deep drop in $u(x)$ and the shorter curves point towards smaller drops in $u(x)$. All curves point towards a zero-crossing of $\mathrm{d}^2/\mathrm{d}x^2 u(x_0)$, and therefore towards points of inflection and drops in $u(x)$. A measure of the importance of these drops is $a_{\max}$, the maximum value of the length scale a reached by the wavelet zero-crossing curve. The length of a wavelet zero-crossing curve $(a_{\max})$ results from both the size of the drop in velocity and the length scale over which this drop is important. Two deep drops that are very close together generate wavelet zero-crossing curves that are also close together.

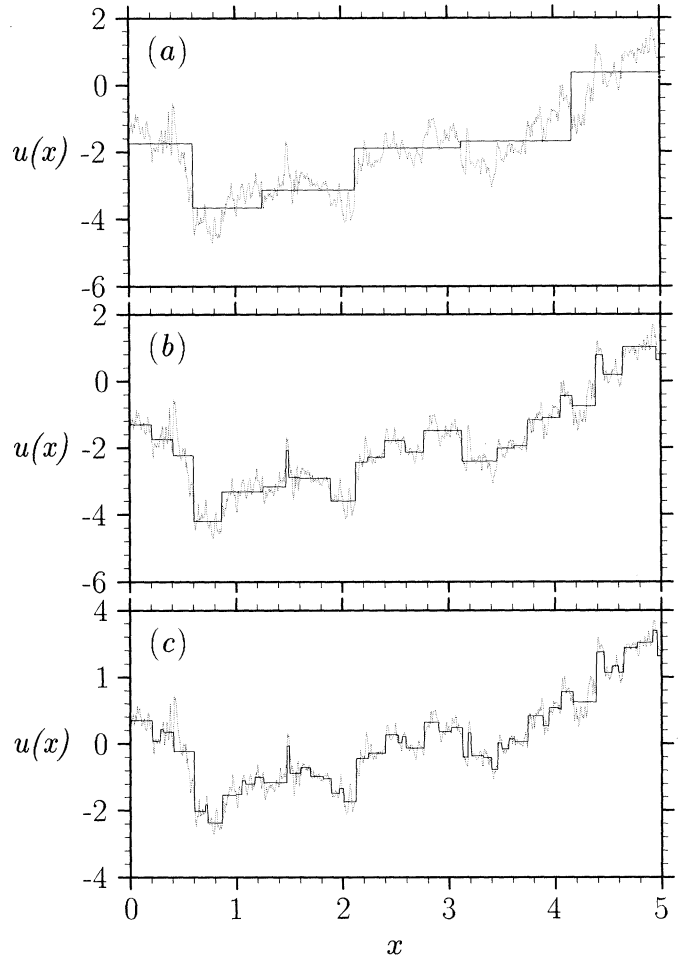

Figure 3. Filtered velocity signal from the zero crossings of the turbulence data in figure 2*b*. (*a*) Scale = 1.0 m. (*b*) Scale = 0.5 m. (*c*) Scale = 0.25 m.

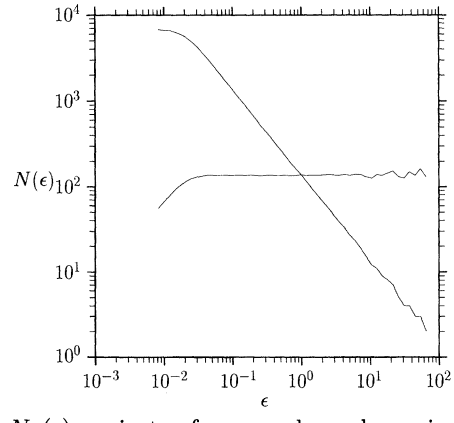

Figure 4. Log-log plot of $N_{\mathrm{E}}(\epsilon)$ against ϵ for a random phase signal with power law energy spectrum $E(k) \propto k^{-5/3}$. Horizontal curve is $\epsilon N_{\mathrm{E}}(\epsilon)$ showing that the eddy capacity $D_{\mathrm{E}} = 1$ and that the signal is space-filling.

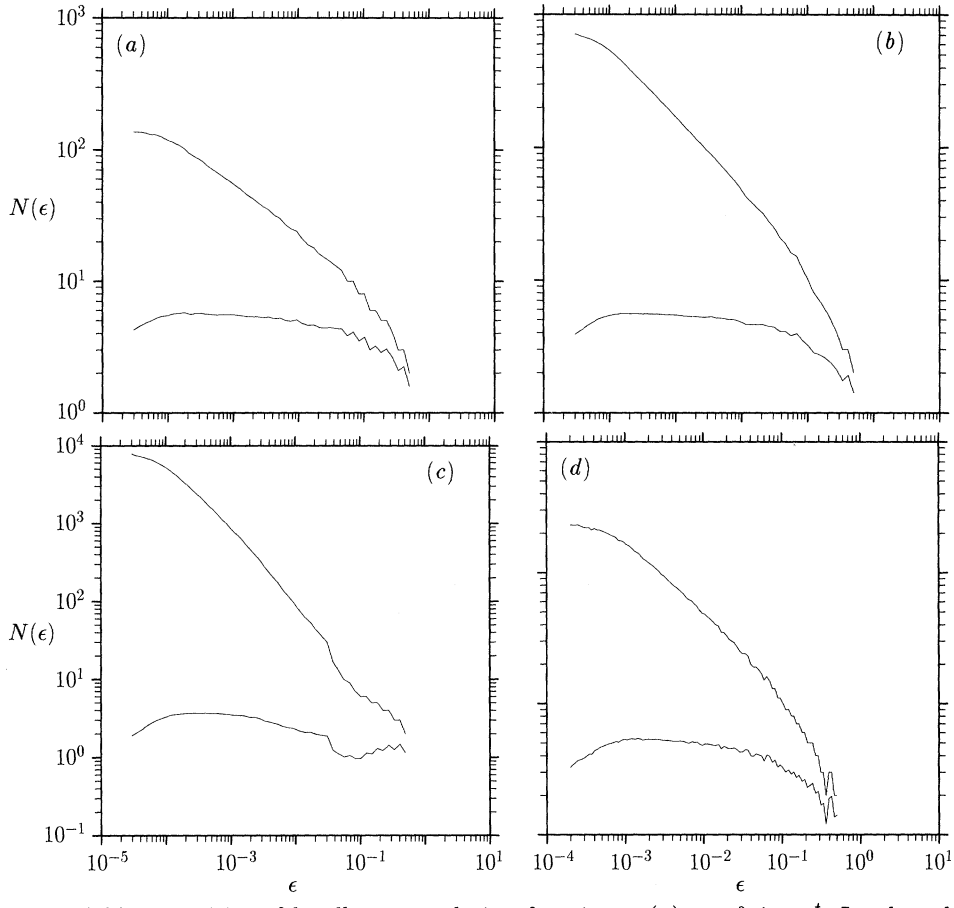

Figure 5. Eddy capacities of locally accumulating functions $u(x) = x^s \sin x^{-t}$. Log-log plots: upper curves are $N_{\mathrm{E}}(\epsilon)$ against ϵ, lower curves are $\epsilon^{D'_{\mathrm{K}}} N_{\mathrm{E}}(\epsilon)$; D'_{K} is the Kolmogorov capacity of the zero crossings for that signal ($D'_{\mathrm{K}} = t/(t+1)$). (*a*) $t = \frac{1}{2}$, $s = 0$, $D_{\mathrm{E}} = 0.367$ (scales 0.0001–0.01). (*b*) $t = 1$, $s = 0$, $D_{\mathrm{E}} = 0.531$ (scales 0.0001–0.01). (*c*) $t = 4$, $s = 0$, $D_{\mathrm{E}} = 0.805$ (scales 0.0001–0.01). (*d*) $t = 1$, $s = 2$, $D_{\mathrm{E}} = 0.530$ (scales 0.0001–0.01).

Given a length scale a, one can construct (Vermeer & Alkemade 1993) a 'blocked' or 'filtered' velocity signal $V_a(x)$ by replacing the original turbulent velocity $u(x)$ with the constant average value of $u(x)$ between every consecutive pair of zero-crossing curves of $a_{\max} \geqslant a$. Figure 3 shows three such wavelet-filtered velocity signals $V_a(x)$ for three different values of a. This construction, or definition, of a turbulence eddy *positions* the eddies along the original turbulence signal. It is only because we define turbulent eddies in terms of wavelet and not Fourier transforms that this positioning is possible.

We would like to think of $V_a(x)$ as only made of eddies of scale a or larger, but some of the fluctuations in figure 3 occur over length scales smaller than a. If these zero-crossing curves are closer than a distance a from each other only one of the two is kept and a filtered velocity field $U_a(x)$ is constructed in the same way as we construct $V_a(x)$, but fast fluctuations over scales smaller than a are neglected, so that $U_a(x)$ *can* be thought of as only made of eddies of scale a or larger.

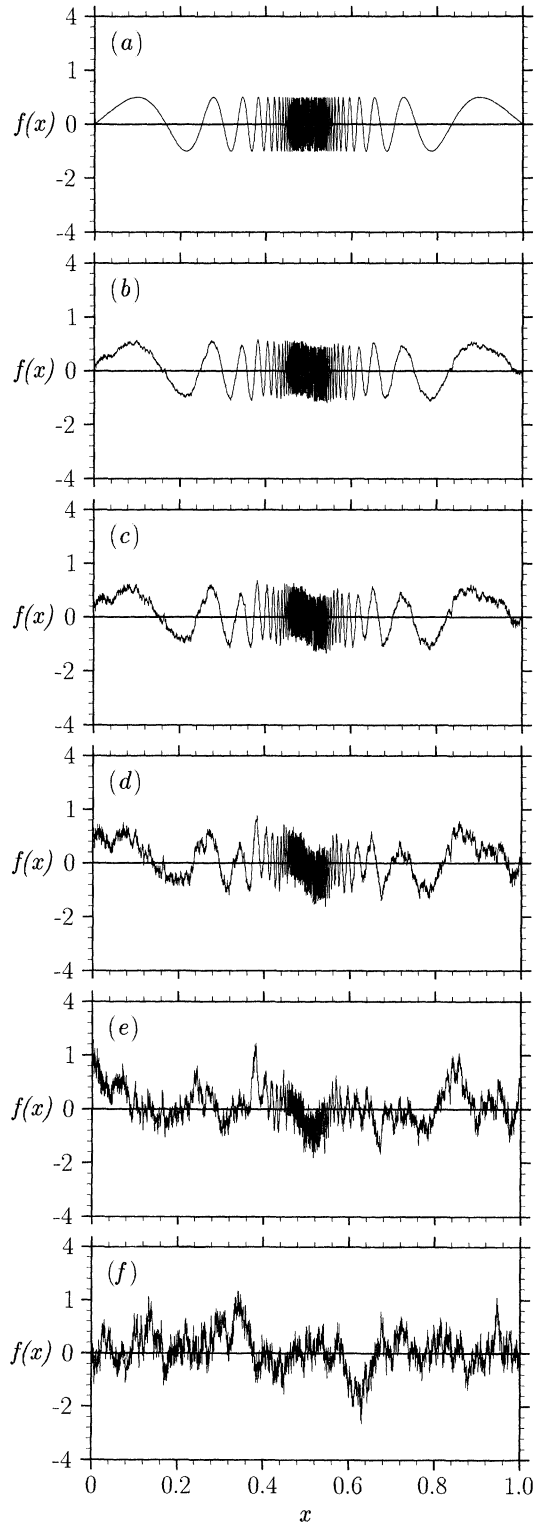

Figure 6. $\sin 2\pi/x$ accumulating function with increasing levels of phase noise. (*a*) 0% noise. (*b*) 5% noise. (*c*) 10% noise. (*d*) 20% noise. (*e*) 40% noise. (*f*) 100% noise.

A measure of the extent to which the spatial distribution of the turbulent eddies of a certain scale a is space-filling, and how this distribution scales with a can be defined in terms of the wavelet zero-crossings. We define $N_{\mathrm{E}}(\epsilon)$: the number of segments of size ϵ that are needed to cover the points x_0 where wavelet zero-crossing curves of $a_{\max} \geqslant \epsilon$ converge as $a \to 0$. A scaling exponent D_{E} is defined if $N_{\mathrm{E}}(\epsilon)$ has a power law dependence on ϵ, in which case†

$$N_{\mathrm{E}}(\epsilon) \sim \epsilon^{-D_{\mathrm{E}}}. \tag{2.2}$$

From our definition of eddies of size larger than a, the number of eddies of size larger than ϵ is proportional to $N_{\mathrm{E}}(\epsilon)$. This is why we call D_{E} the *eddy capacity* of the turbulence: D_{E} is a measure of how the number of eddies varies with their length-scale. An immediate property of D_{E} is that $0 \leqslant D_{\mathrm{E}} \leqslant 1$. $D_{\mathrm{E}} \leqslant 1$ follows from $N_{\mathrm{E}}(\epsilon) \leqslant L/\epsilon$ (where L is the total length of the $u(x)$ record) and D_{E} is non-negative because $N_{\mathrm{E}}(\epsilon)$ cannot increase with ϵ. By definition, if $D_{\mathrm{E}} = 1$ the eddies are space-filling.

A numerical calculation of D_{E} for signals with a random Fourier phase, but a power law energy spectrum shows that $D_{\mathrm{E}} = 1$ irrespective of the power spectrum's scaling $E(k) \sim k^{-2p}$ (see figure 4).

The situation is, however, very different for a locally self-similar signal. A numerical calculation shows that the locally accumulating signal

$$u(x) = x^s \sin x^{-t}, \tag{2.3}$$

where $t > 0$, has an eddy capacity equal to the Kolmogorov capacity: $D_{\mathrm{E}} = D'_{\mathrm{K}}$, for any value of s (where D'_{K} is the Kolmogorov capacity of the zero-crossings of $u(x)$ itself) (see figure 5). In the case of (2.3), $D'_{\mathrm{K}} = t/(t+1)$ (Hunt *et al.* 1993). Idealized functions such as (2.3) are of interest in turbulence and fluid mechanics because they model the velocity, vorticity and scalar fields around a spiral vortex sheet.

The phase spectrum of (2.3) is $\phi_S(k) \sim k^{D'_{\mathrm{K}}}$, and the energy spectrum is $E(k) \sim k^{-2p}$ where $p = 1 + s - (s + \frac{1}{2})D'_{\mathrm{K}}$ provided that $-1 \leqslant 2s \leqslant t$ (Hunt *et al.* 1993). To investigate the effect of varying the amount of phase scrambling we can replace $\phi_S(k)$ by

$$\phi(k) = (1 - f)\phi_S(k) + f\phi_R(k) \tag{2.4}$$

in the Fourier transform of $u(x)$; $\phi_R(k)$ is a random function of wavenumber k and the fraction f is a number between 0 and 1. When f is small, $u(x)$ keeps the accumulating oscillations of (2.3) with superimposed noise only at the larger scales of the 'spiral'. The noise affects the large scales most severely because $\phi(k) \approx (1 - f)\phi_S(k)$ for large k, and thus the random part of the phase spectrum affects only the smaller wavenumbers (see figure 6). Nevertheless, the random part of the spectrum does affect the zero crossings of the wavelet transform at the small scales. As a result, when $f > 0$ there are two ranges of length scales ϵ, (i) the smaller values of ϵ where $D_{\mathrm{E}} = 1$, and (ii) the larger values of ϵ where $D_{\mathrm{E}} = t/(t+1) < 1$ (see figure 7). The noise adds enough zero-crossings to the smaller scales of the wavelet transform to fill the eddy capacity curve out to a

† In a personal communication to the authors, J. G. Jones points out that D_{E} is equivalent to D_2 in Jones *et al.* 1991 since D_2 is found by scaling numbers of *peaks* in the output of a wavelet transform with $\mathrm{d}/\mathrm{d}x \exp(-\frac{1}{2}x^2)$ wavelet, whereas D_{E} is obtained by scaling numbers of *zero-crossings* in the output of the *Mexican hat* wavelet transform.

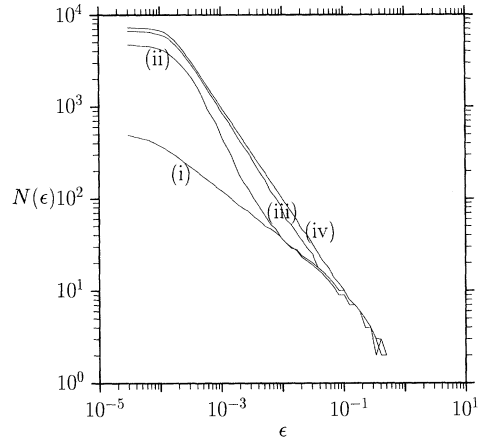

Figure 7. Eddy capacity curves for a $\sin 2\pi/x$ eddy with phase noise levels of (i) 0%, (ii) 0.1%, (iii) 1% and (iv) 50%. With a noise level of 1% the 'eddies' are essentially space filling, $D_{\mathrm{E}} = 1$.

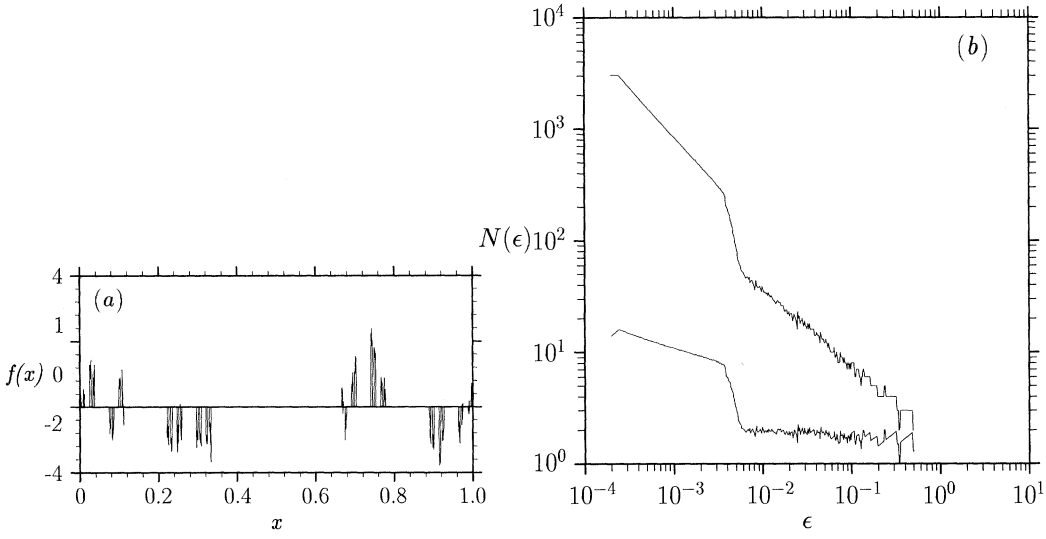

Figure 8. (*a*) Random phase $k^{-5/3}$ signal multiplied by a middle-third Cantor set. (*b*) Eddy capacity curve for the signal in (*a*). The lower curve is $\epsilon^{\log 2/\log 3} N_{\mathrm{E}}(\epsilon)$ and shows that, at the larger scales ϵ, D_{E} is equal to D'_{K} of the Cantor set filter. Here $D'_{\mathrm{K}} = \log 2/\log 3$.

the small scales. As a result, when $f > 0$ there are two ranges of length scales ϵ, (i) the smaller values of ϵ where $D_{\mathrm{E}} = 1$, and (ii) the larger values of ϵ where $D_{\mathrm{E}} = t/(t+1) < 1$ (see figure **??**). The noise adds enough zero-crossings to the smaller scales of the wavelet transform to fill the eddy capacity curve out to a slope of -1 at small ϵ. The range where $D_{\mathrm{E}} = 1$ grows rapidly with f, so that even for small values of f, the scaling appears to be $D_{\mathrm{E}} = 1$ over the entire range; in effect range (ii) becomes vanishingly small and D_{E} is hard to distinguish from 1 even when $f = 0.01$, i.e. 1% phase noise. Thus, a small amount of phase noise can cause a locally accumulating structure to appear space-filling (as defined by D_{E}) at the smaller scales.

If a random phase signal is multiplied by an on-off function that is equal to

Figure 9

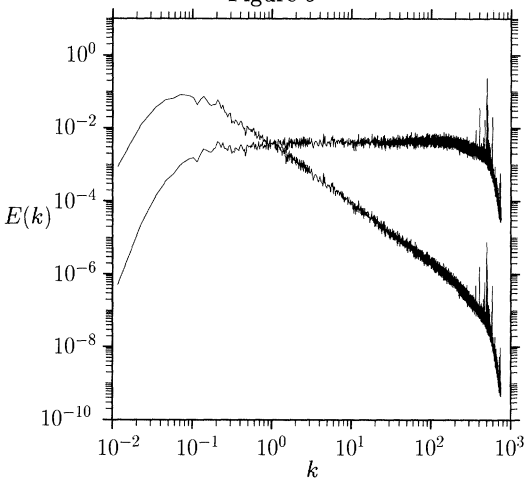

Figure 10

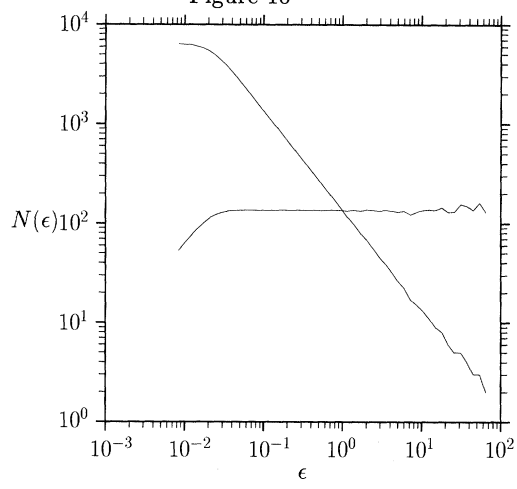

Figure 9. Energy spectrum of the longitudinal velocity component of experimental turbulence (the Taylor hypothesis has been used). Horizontal curve is $\times k^{5/3}$. The large scale part of the spectrum is $\sim k^4$ ($k < 0.04\ \mathrm{m}^{-1}$). The integral scale is at about $k = 7.18\ \mathrm{m}^{-1}$, the Taylor microscale is at $k = 175\ \mathrm{m}^{-1}$ and the Kolmogorov scale (not resolved) is at $k = 18\,000\ \mathrm{m}^{-1}$. The data have been divided into 32 131072 point segments and the Parzen window has been used.

Figure 10. Eddy capacity curve for the longitudinal velocity component of experimental turbulence. The horizontal lower curve is $\epsilon N_{\mathrm{E}}(\epsilon)$, and shows that the turbulence has an eddy capacity, $D_{\mathrm{E}} = 1$.

dimension of the Cantor set (for a Cantor set $D'_{\mathrm{H}} = D'_{\mathrm{K}}$ (Falconer 1990)) in the range of larger length scales that is dominated by the Cantor space structure.

The space-fillingness of eddies defined by $D_{\mathrm{E}} = 1$ is directly sensitive to the phase correlations in $u(x)$. It is the use of the wavelet transform in the definition of D_{E} that provides the way to link space-fillingness to phase correlations. The Hausdorff dimension D'_{H} of the zero-crossings of a random phase signal with Fourier energy spectrum $E(k) \sim k^{-2p}$ is $D'_{\mathrm{H}} = (3 - 2p)/2$ (Orey 1970). The Hausdorff concept of space-fillingness is therefore directly linked to the scaling of the energy spectrum $E(k)$; $D'_{\mathrm{H}} = 1$ when $2p = 1$ and $D'_{\mathrm{H}} = 0$ when $2p = 3$.

In a Fourier decomposition of a signal one specifies the proportion of the total energy that is carried by sine waves of a given wavenumber, i.e. the energy spectrum $E(k)$, and the position of sine waves of different wavenumbers with respect to each other, i.e. the phase spectrum $\phi(k)$. These two distinct specifications relate to two different concepts of space-fillingness and self-similarity based on, respectively, D'_{H} and D_{E}. D'_{H} measures the relative proportion of energy in different wavenumbers: the greater the proportion of energy in the higher wavenumbers, the more irregular the signal. Hence, D'_{H} is a measure of a space-fillingness that is equivalent to irregularity. However, a signal that is not very irregular can have $D_{\mathrm{E}} = 1$ provided the phases are decorrelated. When the phases are correlated enough for $u(x)$ to have an identifiable space structure, $D_{\mathrm{E}} < 1$, indicating that turbulent eddies are not uniformly distributed in space relative to each other. D_{E} is a scaling exponent that is sensitive to the scaling and space-fillingness in real space, whereas D'_{H} is a scaling exponent that is sensitive to the scaling and space-fillingness in wavenumber space.

The eddy capacity was calculated for the experimental longitudinal turbulence data from the Modane wind tunnel provided by Gagne (1987). The data has the following characteristics: a Taylor microscale based Reynolds number of 2720, the mean speed is 20.8 m s^{-1}, and sampling frequency is 5000 Hz (giving a Taylor hypothesis spatial resolution of 0.00416 m). The Taylor microscale, λ, is 0.036 m; the Kolmogorov scale, η_K, is 0.00035 m and the integral scale is approximately 2500× the Kolmogorov scale. The turbulence energy spectrum exhibits a well defined scaling law that is close to the Kolmogorov $-\frac{5}{3}$ law (see figure 9). The $E(k) \sim k^{-5/3}$ inertial range extends over nearly three decades, from the integral length scale to somewhere between λ and the Kolmogorov scale η_K. Even though the turbulence data we use has a very high Reynolds number (one of the highest to date achieved in the laboratory), η_K is not adequately resolved. The eddy capacity of this experimental turbulence data (e.g. figure 2*b*) is $D_E = 1$ over a range of length scales between the integral length scale of the turbulence and slightly above the Taylor microscale λ (see figure 10).

The result $D_E = 1$ indicates a certain degree of phase decorrelation in the inertial scales of turbulent motion above the Taylor scale λ. In a recent study of DNS isotropic turbulence, Vassilicos *et al.* (1993) find well-defined scalings of the smooth geometry of streamlines around the vortex tubes that dominate the range of scales below λ. As pointed out by Lundgren (1993), Moffatt (1993) and Hunt & Vassilicos (1991), if these vortex tubes represent singularities, such as rolled up vortex sheets, they should contribute to the scaling of $E(k) \sim k^{-5/3}$ as well. Yet, the advection (whether chaotic or not (Ottino 1989; Vassilicos & Fung 1994)) of the small-scale vortex tubes by the ambient unsteady velocity field can influence the scaling laws of the turbulence (Malik & Vassilicos 1994) and may also be partly responsible for the weak phase correlations of the 1D turbulence signal $u(x)$ above λ. Below λ the phase correlations may not be weak if the motion is dominated by the structure of vortex tubes. A phase scrambled signal is globally self-similar. It is important to unravel the components of the turbulence that carry or cause a local or a global self-similarity in various turbulence scalings (Vassilicos & Hunt 1991). In the following section we address the question of whether the smaller inertial scales of motion are locally or globally self-similar and develop a practical test which we apply to the inertial scales of the 1D turbulence signal below λ.

3. The self-similarity of the smaller inertial scales

Do the small scales of turbulence have a local or a global self-similarity? In this section we introduce a method of distinguishing between locally and globally self-similar signals based on differences in the distribution of singularities in each type of signal.

If a stochastic signal $u(x)$ has globally self-similar scaling, then $u(x)$ carries a *dense* set of singularities and has accumulating length scales everywhere (Vassilicos & Hunt 1991). The wavelet transform of such a signal is shown in figure 11*a*, and is characterized by long slender conical structures that point towards the x_0 axis in the direction where $a \to 0$. The wavelet transform of an isolated singularity has a single conical structure; the wavelet transform of a signal with a dense set of singularities should have a dense number of cones pointing towards

the x_0 axis (Hunt *et al.* 1993). The average wavelet transform $\tilde{U}(x_0, a)$ of the wavelet transforms $\tilde{u}_r(x_0, a)$ of N different realizations $u_r(x)$ $(r = 1, 2, \ldots, N)$ of the stochastic signal should have no cones. A superposition of a dense number of conical structures of random sign should produce cancellations of the conical structures everywhere.

If on the other hand the stochastic signal $u(x)$ has a locally self-similar scaling, then $u(x)$ carries a *sparse* set of isolated singularities. Figure 11*b* shows the single cone produced by a single locally accumulating function. In this case, an averaging of the wavelet transforms $\tilde{u}_r(x_0, a)$ of N different realizations $u_r(x)$ $(r = 1, 2, \ldots, N)$ may not result in a cancellation of the cones. Instead, we expect $\tilde{U}(x_0, a)$ to be the collection of the cones in all realizations simply because the likelihood that two cones from two different realizations coincide is practically zero when the set of singularities is sparse. A sparse set of singularities implies a collection of cones, whereas a dense set of singularities implies a cancellation of cones in the wavelet transform.

Let us develop this distinction between locally and globally self-similar signals by way of examples.

(i) A single realization $u_r(x)$ of a random phase signal can be written

$$u_r(x) = \int |\hat{u}(k)| \exp(\mathrm{i}\phi_r(k)) \exp(-\mathrm{i}kx)\, \mathrm{d}k, \tag{3.1}$$

in terms of the modulus† $|\hat{u}(k)|$ of its Fourier transform $\hat{u}(k)$ and of a realization of the random phase spectrum $\phi_r(k)$. Thus each realization has the same distribution of energy in wavenumber space, but different phases. The wavelet transform $\tilde{u}_r(x_0, a)$ of $u_r(x)$ can also be calculated in Fourier space (Hunt *et al.* 1993);

$$\tilde{u}_r(x_0, a) = a^{-1/2} \int |\hat{u}(k)| \exp(\mathrm{i}\phi_r(k)) \hat{\psi}^*(ak) \exp(-\mathrm{i}kx_0)\, \mathrm{d}k, \tag{3.2}$$

where $\hat{\psi}$ is the Fourier transform of the 'mother' wavelet ψ. The average $\tilde{U}(x_0, a)$ of the wavelet transforms of N realizations is

$$\tilde{U}(x_0, a) = \frac{1}{N} \sum_{r=1}^{N} \tilde{u}_r(x_0, a), \tag{3.3}$$

and it follows that

$$\tilde{U}(x_0, a) = a^{-\frac{1}{2}} \int \mathrm{d}k |\hat{u}(k)| \hat{\psi}^*(ak) \exp(-\mathrm{i}kx_0) \frac{1}{N} \sum_{r=1}^{N} \exp(\mathrm{i}\phi_r(k)). \tag{3.4}$$

Because the phases $\phi_r(k)$ are random numbers between $-\pi$ and $+\pi$, the sum $\sum_{r=1}^{N} \exp(\mathrm{i}\phi_r(k))$ is essentially equivalent to a random walk, and there exists a random function $\phi'(k, N)$ such that

$$\sum_{r=1}^{N} \exp(\mathrm{i}\phi_r(k)) \approx \sqrt{N} \exp(\mathrm{i}\phi'(k, N)), \tag{3.5}$$

† To imitate equilibrium turbulence one may choose $|\hat{u}(k)| \propto k^{-5/6}$.

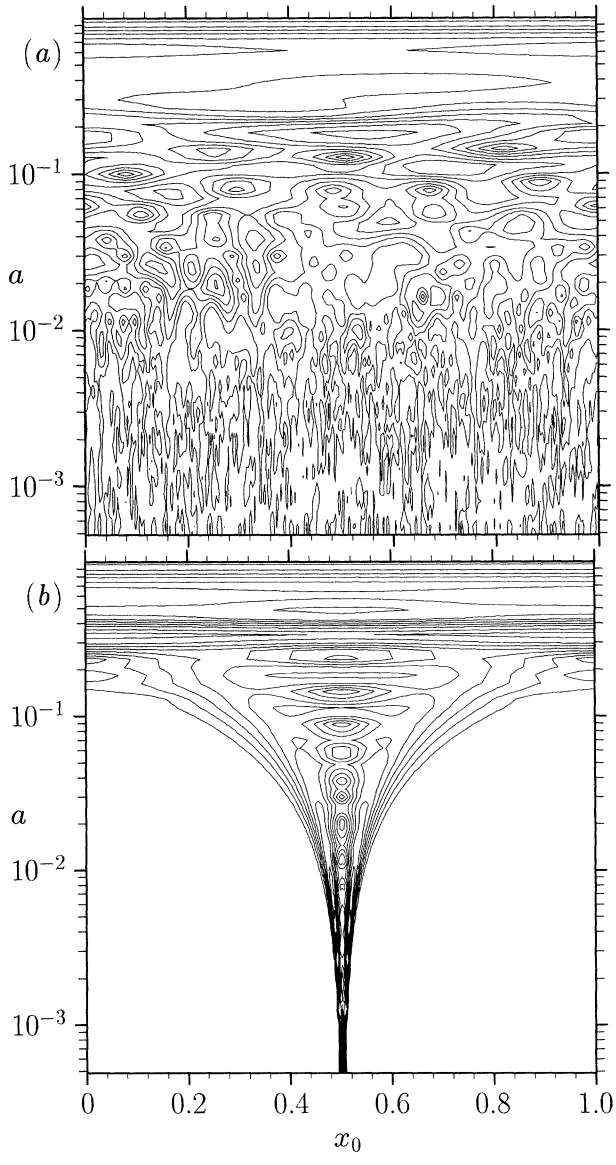

Figure 11. (*a*) Morlet wavelet transform of a random phase signal with energy spectrum $E(k) \propto k^{-5/3}$. (*b*) Morlet wavelet transform of $\sin(2\pi x^{-1/2})$ ($E(k) \propto k^{-5/3}$).

if N is large enough. Therefore,

$$\tilde{U}(x_0, a) \approx \frac{a^{-1/2}}{\sqrt{N}} \int |\hat{u}(k)| \hat{\psi}^*(ak) \exp(-\mathrm{i}kx_0) \exp(\mathrm{i}\phi'(k, N)) \, \mathrm{d}k, \tag{3.6}$$

which means that $\tilde{U}(x_0, a)$ is equal to one particular realization of the wavelet transform $\tilde{u}_r(x_0, a)$ divided by $\sqrt{N}$.

The cones are the regions in (x_0, a) space where most of the 'wavelet energy' $|\tilde{u}(x_0, a)|^2$ concentrates. The cone structure in $\tilde{U}(x_0, a)$ is qualitatively the same

as in $\tilde{u}_r(x_0, a)$, but weaker by a factor $\sqrt{N}$. Random phase signals are globally self-similar and their singularities are dense. Indeed an averaging over many realizations of such signals removes, gradually, the cone structure in the wavelet transform.

Let us define σ_w, the integral over all locations of the modulus of the wavelet transform,

$$\sigma_w(a) = \int |\tilde{U}(x_0, a)| \, \mathrm{d}x_0. \tag{3.7}$$

$\sigma_w(a)$ is large if either many or strong (or both many and strong) cones cross the coordinate a in the wavelet plane (x_0, a) (by 'strong' we mean energetic). From (3.6) we see that $\sigma_w(a) = O(N^{-\frac{1}{2}})$ for random phase signals. This result is confirmed numerically at several different scales in figure 12*a*.

These properties are not unique to random phase signals, but also appear in other globally self-similar signals such as the Weierstrass function (Falconer 1990). In figure 12*b* $\sigma_w(a)$ is plotted as a function of the number of realizations, and again $\sigma_w(a)$ at each scale decreases like $O(N^{-\frac{1}{2}})$ with the number of realizations N.

(ii) Now consider a locally accumulating signal. A single realization of a 'spiral' function

$$x^s \exp(\mathrm{i}x^{-t}) H(x) \tag{3.8}$$

(where $H(x)$ is the Heaviside function) is

$$u_r(x) = (x - c_r)^s \exp(\mathrm{i}(x - c_r)^{-t}) H(x - c_r), \tag{3.9}$$

where c_r is the centre of the spiral (a random number between, say, 0 and 1). The 'spiral' function is an isolated (and therefore sparse) singularity and is locally self-similar since it has a local accumulation of length scales towards the centre, c_r, of the spiral. The Kolmogorov capacity of the zero-crossings of $u_r(x)$ is $D'_{\mathrm{K}} = t/(t+1)$, but the Hausdorff dimension $D'_{\mathrm{H}} = 0$.

If the Morlet 'mother' wavelet $\psi(x) = \exp(-\frac{1}{2}x^2)\exp(\mathrm{i}x)$ is used, by a trivial change of variables the wavelet transform of (3.9) is

$$\tilde{u}_r(x_0, a) = a^{-1/2} \int_0^{+\infty} x^s \exp\left(\mathrm{i}\left(x^{-t} + \frac{x - x_0 + c_r}{a}\right)\right) \exp\left(-\frac{(x - x_0 + c_r)^2}{2a^2}\right) \mathrm{d}x. \tag{3.10}$$

This integral can been estimated in the limit $a \to 0$ by the method of stationary phases (Hunt *et al.* 1993). One finds that

$$\tilde{u}_r(x_0, a) \sim a^{p-1/2} \exp\left(-\frac{(x_0 - c_r - (ta)^{1/(t+1)})^2}{2a^2}\right) \times \exp\left(\mathrm{i}\left[(1+t)(ta)^{-t/(t+1)} - \frac{x_0 - c_r}{a}\right]\right) \tag{3.11}$$

as $a \to 0$, where $p = (2s + t + 2)/(2(t+1))$. If we define $\tilde{u}_0(x_0, a)$ to be equal to $\tilde{u}_r(x_0, a)$ when $c_r = 0$, the average wavelet transform $\tilde{U}(x_0, a)$ is

$$\tilde{U}(x_0, a) \sim \tilde{u}_0(x_0, a) \frac{1}{N} \sum_{r=1}^{N} \exp\left(\mathrm{i}\frac{c_r}{a}\right) \exp\left(-\frac{c_r^2}{2a^2}\right) \exp\left(\frac{c_r}{a^2}(x_0 - (ta)^{1/(t+1)})^2\right), \tag{3.12}$$

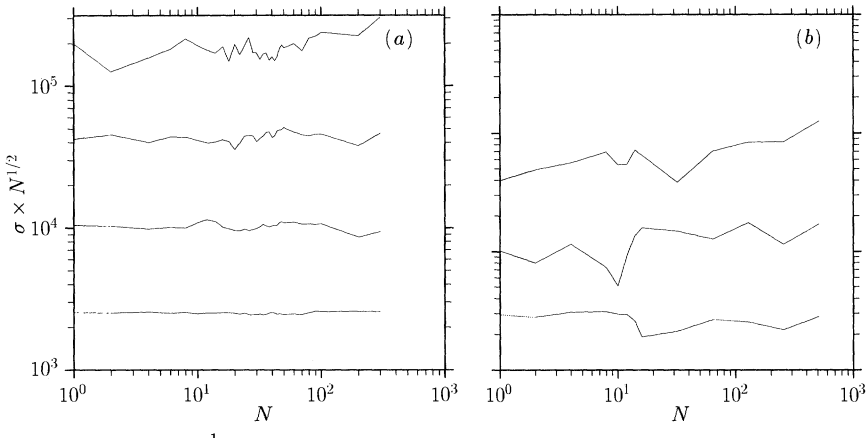

Figure 12. (*a*) $\sigma_w(a) \times N^{\frac{1}{2}}$ of a random phase signal as a function of number of realizations at scales $a = 1.94 \times 10^{-2}$, 0.106, 0.575, 3.13 (from bottom). (*b*) $\sigma_w(a) \times N^{\frac{1}{2}}$ of a Weierstrass function ($f(x) = \sum_{k=1}^{\infty} \lambda^{(s-2)k} \sin(\lambda^k t)$, $\lambda = 1.5$, $s = 1.5$, the series is truncated after the first 50 terms) as a function of number of realizations at scales $a = 1.14 \times 10^{-3}$, 6.20×10^{-3}, 0.0337 (from bottom).

and a numerical computation of the sum in (3.12) leads to

$$\sum_{r=1}^{N} \exp\left(\mathrm{i}\frac{c_r}{a}\right) \exp\left(-\frac{c_r^2}{2a^2}\right) \exp\left(\frac{c_r}{a^2}(x_0 - (ta)^{1/(t+1)})^2\right) \approx NF(x_0, a) \qquad (3.13)$$

for large enough values of N. It then follows that $\tilde{U}(x_0, a)$ is asymptotically independent of N as $N \to +\infty$.

It is clear from figure 13 that the number of wavelet cones in the structure of $\tilde{U}(x_0, a)$ increases proportionally with N, but it is also clear that the cones become shorter as N increases. The width of the cones is larger at larger length scales a, and thus the cones superimpose and cancel at these scales. However, at the smaller scales the cones do not cancel because the self-similar singularities remain isolated and sparse. At these small scales, $\sigma_w(a)$ is independent of N (figure 4). The scales where $\sigma_w(a)$ is independent of N also become progressively smaller as N increases. In the case of the Morlet wavelet transformed spiral, the width of the cone $l(a) \propto a$. Indeed, in equation (3.11), $\tilde{u}_r(x_o, a)$ is proportional to a gaussian of width a. Thus, the thin ends of the cones will, on average, not cancel where $a < L/N$ (where L is the length of the data segment and N is the number of realizations).

The result that $\sigma_w(a)$ is independent of N follows from equation (3.11) which is valid with the restriction that $a \to 0$. Additionally, from the above argument, the scales where this effect is visible decrease with number of realizations N. For this method of distinguishing between local and global self-similar structure to work in practise we therefore need a turbulence velocity signal with an extremely large range of length scales.

A question may also be asked about the robustness of this method: how sensitive is it to the amount of noise in the signal? We have already seen that the eddy capacity D_{E} is very sensitive to even small amounts of phase noise. Figure 15 shows that the present method is relatively insensitive to phase noise. Even at

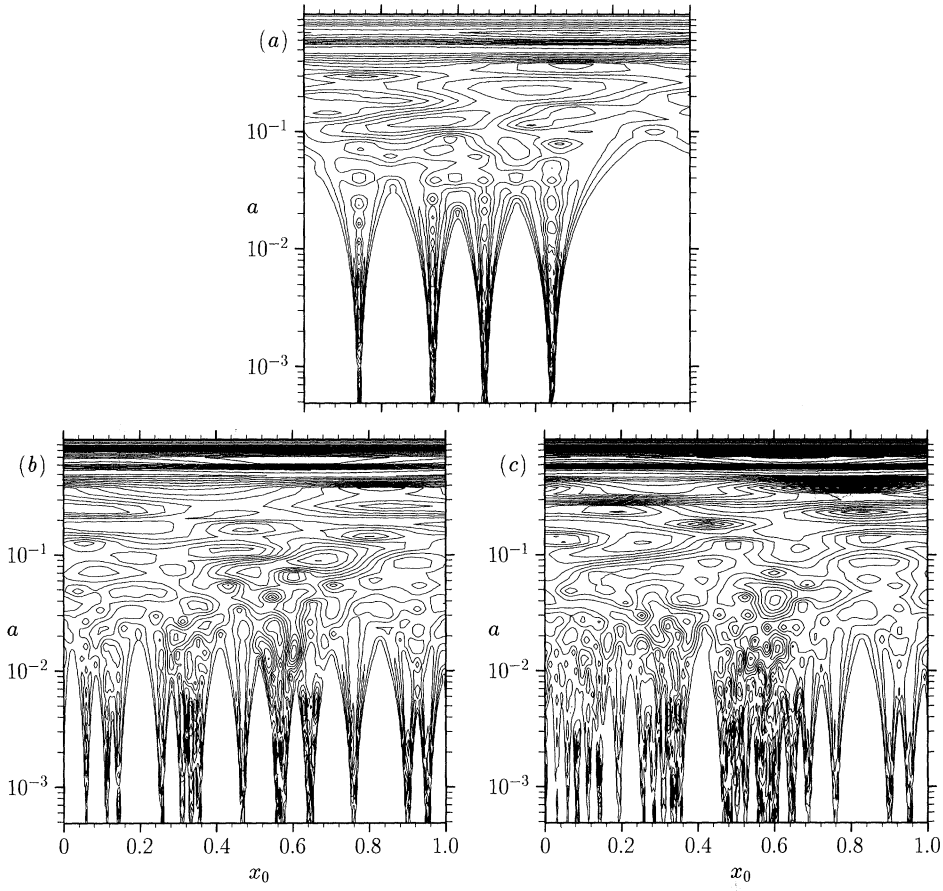

Figure 13. Modulus of the Morlet average wavelet transform of (*a*) 4, (*b*) 16 and (*c*) 32 spirals showing the cone structure. Note how at the smaller scales the cones accumulate and do not cancel.

40% phase noise σ_w is still significantly different from the $N^{-\frac{1}{2}}$ random phase behaviour for $N < 10$. This is a useful result since most turbulent spirals will have some degree of noise (deviation from a perfectly accumulating structure) and shows that this method should be useful in practise.

To summarize, the method is to wavelet transform successive stretches of at least one Taylor microscale in the turbulence signal. Then we collect the wavelet transforms of N 'realizations' of small-scale turbulence structure and average them together to obtain $\tilde{U}(x_0, a)$ and $\sigma_w(a)$. (In practise this is equivalent to averaging out the 'realizations' first and then wavelet transforming the average signal, because averaging and wavelet transforming are both linear operations and therefore commute.) If $\sigma_w(a)$ decreases like $N^{-\frac{1}{2}}$ over all length scales a then the turbulence is *H-fractal*; if, on the contrary, $\sigma_w(a)$ is independent of N at small values of a, then the signal is *K-fractal* and may carry spiral singularities.

Figure 16*a* shows the Morlet wavelet transform of the first 512 points of the experimental turbulence data described above. The figure shows strong cone-like branching at $x = 0.40$ m and $x = 1.60$ m which may be the result of locally self-similar structures (compare with the actual velocity trace in figure 16*b*). In

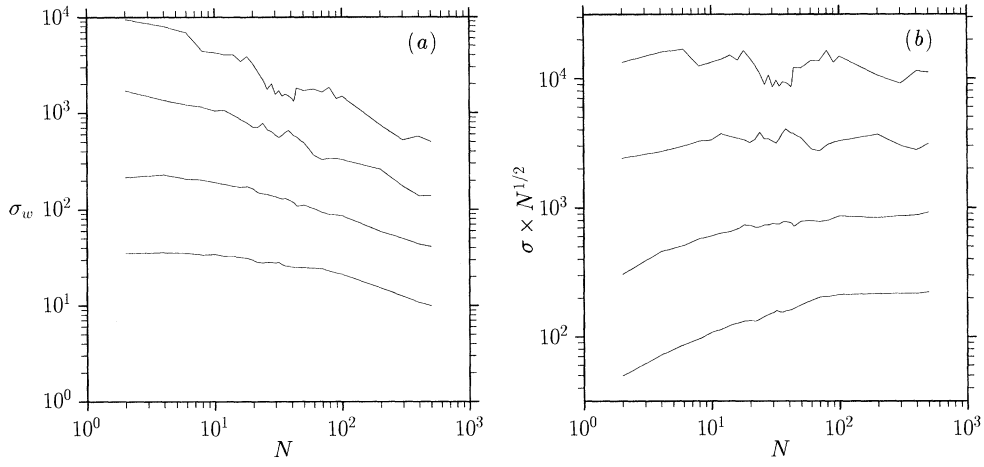

Figure 14. (*a*) $\sigma_w(a)$ at scales $a = 1.94\times10^{-2}$, 0.106, 0.575, 3.13 for the 'spiral' function $\sin(x^{-\frac{1}{2}})$. (*b*) Same as (*a*), but $\times N^{\frac{1}{2}}$. Note how $\sigma_w(a)$ remains approximately constant at small scales and moderate N, and becomes more like a random phase signal (decreasing like $N^{-\frac{1}{2}}$) at large scales and large N.

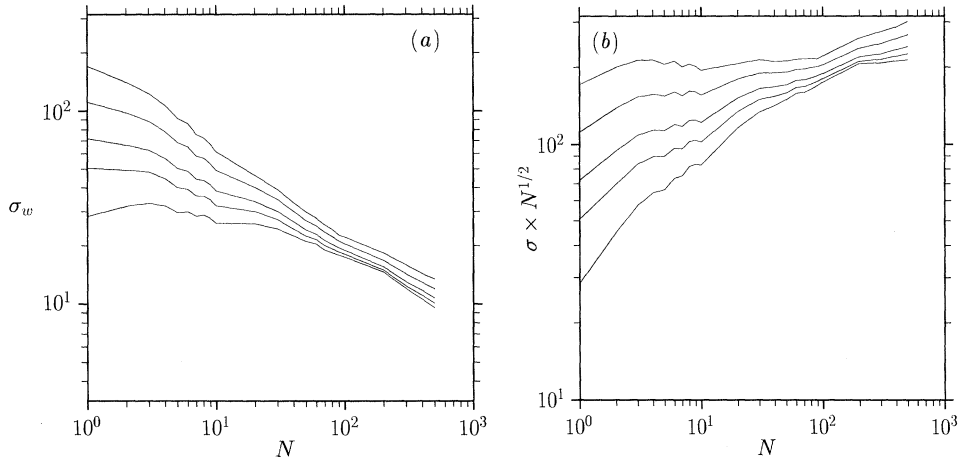

Figure 15. (*a*) $\sigma_w(a)$ at a single scale for levels of noise 0%, 5%, 10%, 20% and 40% (from bottom). (*b*) Same as (*a*), but $\times N^{\frac{1}{2}}$.

figure 17*a* σ_w indicates H-fractal ($\sigma_w \sim N^{-\frac{1}{2}}$) behaviour at all scales for large 17.0 m data segments (4096 points). For smaller 0.133 m segments (about four Taylor microscales) figure 17*b* shows no $\sigma_w \sim N^{-\frac{1}{2}}$ behaviour for $N < 10$ and some faint evidence of K-fractal behaviour. As mentioned above, evidence of K-fractal behaviour is expected to disappear eventually with increasing N because of the data's finite resolution.

Averaging segments much larger than λ may reduce existing K-fractal traces if the lateral size of the small-scale turbulence vortex tubes, assumed to have a spiral internal structure, is $O(\lambda)$. Segments much longer than λ would then include many spirals, thereby effectively increasing N. Note that the 17.0 m long segments are about 486 λ long. Unfortunately, the Taylor microscale and below

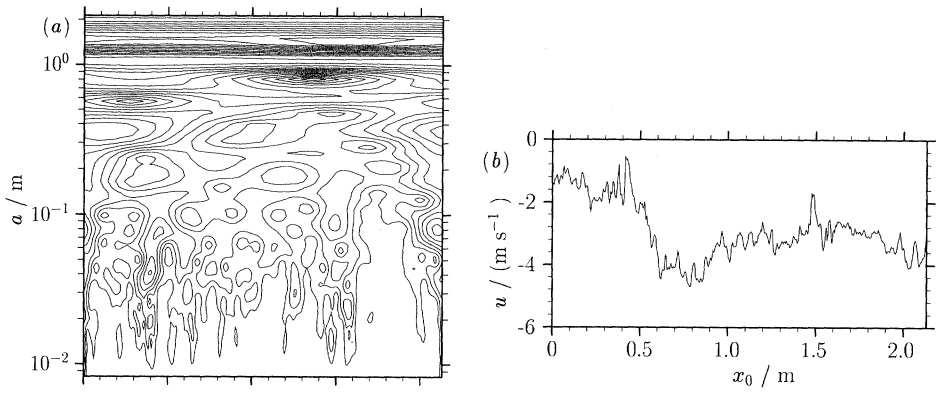

Figure 16. (*a*) Morlet wavelet transform of first 512 points of experimental turbulence data (longitudinal velocity component). (*b*) Original signal. Note branching and especially strong cones at $x = 0.40$ m and $x = 1.60$ m.

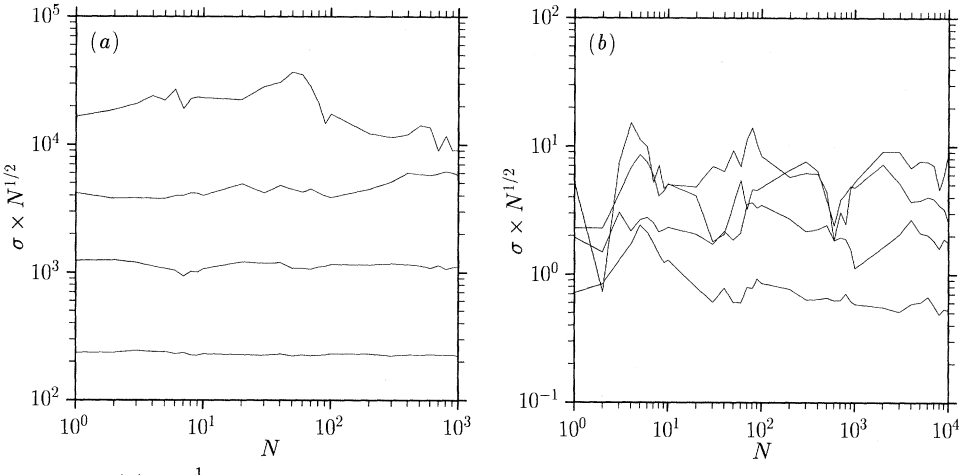

Figure 17. $\sigma_w(a) \times N^{\frac{1}{2}}$ as a function of number of realizations. (*a*) 4096pt (17.0 m) long segments (scales 1.94×10^{-2}, 0.106, 0.575, 3.13 m). (*b*) $\sigma_w(a) \times N^{\frac{1}{2}}$ for 32pt (0.133 m) long segments (scales 1.10×10^{-2}, 2.03×10^{-2}, 3.76×10^{-2}, 6.96×10^{-2}). Note the deviation from the H-fractal $N^{-\frac{1}{2}}$ slope for $N < 10$.

are not resolved well enough to provide strong evidence of K-fractal behaviour, although some evidence of non H-fractal behaviour does exist for averages of less than 10 realizations. Furthermore, the number of spiral events captured in the velocity data may be low because the probability of a single point probe intersecting a line vortex is small.

4. Spatial fluctuations of wavelet energy

Thus far we have introduced two new methods for analysing the self-similar structure of turbulence. The first method uses the zero crossings of the wavelet transform to define an eddy capacity which is a measure of the space-fillingness of the signal in real space and the second method uses differences in the cancellation of energy in averaged wavelet transformed signals to distinguish between local and

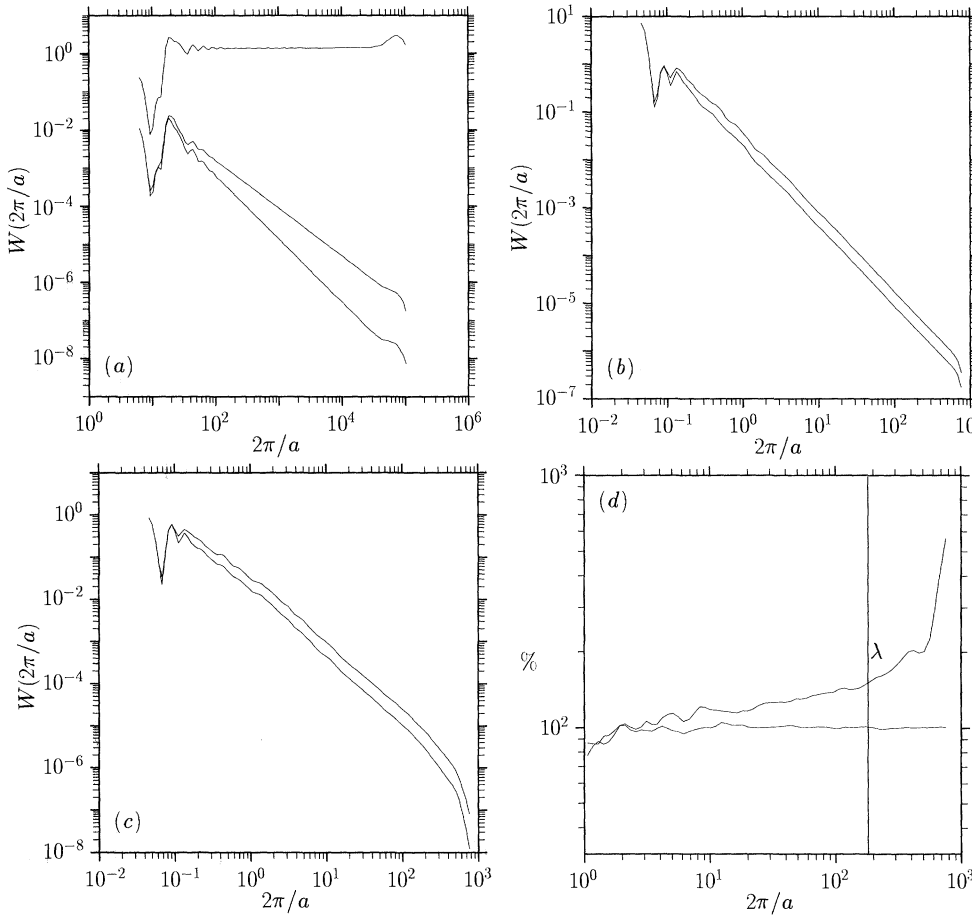

Figure 18. Spatial fluctuation of wavelet energy (average of 50 realizations). (*a*) $\sin(t^{-1/2})$ spiral. Lower curve is wavelet energy spectrum, middle curve is plus one standard deviation and upper curve is the wavelet spectrum $\times a^{-5/3}$. (*b*) Random phase signal ($E(k) \propto k^{-5/3}$). Lower curve is wavelet energy spectrum, upper curve is plus one standard deviation. (*c*) Experimental turbulence data. Lower curve is wavelet energy spectrum, upper curve is plus one standard deviation. (*d*) Percent standard deviation of wavelet energy spectrum ($I(a)$). Top curve is the experimental turbulence data, lower curve is the random phase signal, λ indicates the Taylor microscale.

global self-similar structures. In this section we again use the wavelet transform, but now the magnitude of the fluctuations of the wavelet energy is measured as a function of scale. The standard deviation of the wavelet energy is defined as

$$I(a) = \left[\int_0^L (\tilde{u}^2(x_0, a) - W(a))^2 \, \mathrm{d}x_0\right]^{\frac{1}{2}} / W(a), \tag{4.1}$$

where $W(a)$ is the wavelet energy averaged over all locations,

$$W(a) = \frac{1}{L}\int_0^L \tilde{u}^2(x_0, a) \, \mathrm{d}x_0. \tag{4.2}$$

$I(a)$ is a measure of the deviation of the local wavelet energy from its spatial

mean. A large value of $I(a)$ indicates that the energy of the turbulence at scale a varies greatly from place to place in the flow (high energy fluctuation), while a small value of $I(a)$ indicates the energy is essentially the same at all locations (and hence that the Fourier energy spectrum is a good representation of the local energy scaling). Note that $I(a)$ is large for highly intermittent turbulence, although the converse is not necessarily true. This means that the standard deviation of the wavelet energy can be a misleading measure of intermittency.

Meneveau (1991) found a high deviation (of the same magnitude as the energy itself) of wavelet energy in both experimental and DNS turbulence flows. He also found that the deviation increases slightly at the smaller lengthscales, indicating greater fluctuations at the smaller scales. The particular question we wish to address here is: how much and what aspects of these fluctuations are due to small-scale local structures in the flow and how much are due to the phase scrambling of the turbulence at the larger inertial scales? As in § 3 the question is about the relative roles of the global and local parts of the inertial range of turbulence.

The signals analysed in this section have the same power law exponent for both the Fourier and wavelet energy spectrum. In figure 18*a* the wavelet energy spectrum of a locally self-similar spiral signal $\sin(x^{-\frac{1}{2}})$ is compared to the same wavelet energy spectrum plus one standard deviation. The deviation is very small at the largest scales but then increases steadily with $1/a$. The random phase signal (figure 18*b*) also shows little fluctuation at the large scales. However, after about $1/a = 1$ the standard deviation remains constant at a magnitude about equal to that of the wavelet energy spectrum. Figure 18*c* shows the wavelet energy spectrum alone and plus one standard deviation of the experimental turbulence data. The turbulence data shows an increase in fluctuation with $1/a$ somewhat less than that of the single spiral, but significantly more than that of the random phase signal. The difference between the random phase and turbulence signal is brought out strongly in figure 18*d* which compares $I(a)$ of the turbulence and random phase signals. The fluctuation of the random phase signal remains constant at 100% down to the smallest lengthscales, whereas the fluctuation of the turbulence signal *increases* with $1/a$. The fluctuation becomes very large around the Taylor microscale λ. It is interesting to note that the approximate magnitude of standard deviation of energy measured by Meneveau (100%) is the same as that measured from the random phase $k^{-5/3}$ signal. This suggests that the overall level of energy fluctuation is actually set by the phase-scrambled larger scale part of the inertial range turbulence, and is not, therefore, a significant measure of intermittency. However, the *increase* in energy fluctuations at small scales may reflect the presence of local coherent structures.

5. Concluding remarks

This paper has introduced a new statistical eddy based on the zero crossings of the Mexican Hat wavelet transform and an associated dimension, the eddy capacity D_{E}. D_{E} is a measure of the scaling and space-fillingness of the distribution of turbulent eddies in physical space. For an intermittent H-fractal distribution of eddies, $D_{\mathrm{E}} < 1$ over the range of length scales that characterize the intermittency, and is equal to the Kolmogorov capacity D'_{K} of the spatial distribution of intermittent activity. If the H-fractal distribution of eddies is not intermittent,

$D_E = 1$, thus revealing the *space-fillingness of eddies in physical space.* However, D'_K and D'_H may be both smaller than 1, and their value is a function of the energy spectrum. If the energy is maximally distributed over all wavenumbers, i.e. $E(k) \sim k^{-1}$ (since the total energy is infinite when $E(k) \sim k^{-2p}$ with $2p \leqslant 1$), then $D'_K = D'_H = 1$, thus reflecting the *space-fillingness in wavenumber space.* Space-fillingness in the physical and wavenumber spaces are not equivalent concepts, the scaling exponent D_E being a measure of the former, while the scaling exponents D'_K and D'_H are measures of the latter.

For a K-fractal distribution of eddies, such as may occur in a spiral vortex sheet, $D_E = D'_K$ and $D'_H = 0$. Our results have shown that D_E determines the scaling of the phase spectrum uniquely in this case, but not the energy spectrum. $D_E = 1$ when the phases are the same over all wavenumbers or when they are random, which is the way the phase spectrum reflects space-fillingness in the physical space. $D_E = 1$ at the larger inertial scales of the turbulent longitudinal velocity signal, thereby indicating a degree of phase decorrelation at the larger inertial scales.

A practical method of distinguishing between local and global self-similarity has been introduced. This technique exploits differences in the way the average of the wavelet transforms of many realizations decays with N (the number of realizations). It is shown that the average wavelet transform decays like $N^{-\frac{1}{2}}$ for random phase signals and Weierstrass functions (globally self-similar), while for spiral-like signals (locally self-similar) the average wavelet transform does not decay! The turbulence data shows some very faint (at this stage, inconclusive) evidence of spiral-type structure. The lack of resolution of our data below the Taylor microscale λ prevents firm conclusions.

Following Meneveau (1991) the fluctuation of the energy is measured by calculating the spatial standard deviation of the wavelet energy as a function of scale. The spatial fluctuations of a random phase signal, spiral signal and experimental turbulence signal (all with $E(k) \propto k^{-5/3}$) are calculated. It is found that the fluctuation is very small at the largest scales in all three cases. The random phase signal's fluctuation remains independent of scale as scale decreases, while the fluctuation of the spiral signal increases steadily with $1/a$. The magnitude of energy deviation of the turbulence data is about the same as the random phase signal, but it increases with $1/a$ like the spiral signal. The level of energy fluctuation is set by the phase scrambled part of the inertial range, but the *increase* of fluctuation with wavenumber must be due to some form of phase organisation. This phase correlation is linked to intermittency and may be the result of small scale coherent flow structures.

While the energy spectrum of the turbulence appears to scale uniformly like $k^{-5/3}$ over the entire inertial range, our results suggest that the corresponding scaling of the turbulent 1D velocity signal in physical space changes qualitatively from an H-fractal scaling at the larger inertial scales to a K-fractal scaling at the smaller inertial scales. This picture agrees with and adds a scaling aspect to the idea that the turbulence is a collection of small-scale coherent locally self-similar flow structures in a surrounding larger scale H-fractal sea, where the turbulence is phase-scrambled to a degree (e.g. how large is f in (2.4)?) that we are unable to determine in the present study.

We are grateful to Tony Fincham and Tom Gilmour of British Gas plc for allowing us to use

the wavelet zero-crossings algorithm that British Gas uses in the study of pipe corrosion. We are also grateful to Yves Gagne for providing the Modane turbulence data, and to Glynn Jones who read the manuscript and gave many very useful suggestions for improvement. This work was funded by British Gas.

References

Batchelor, G. K. 1953 *Homogeneous turbulence.* Cambridge University Press.

Falconer, K. 1990 *Fractal geometry—mathematical foundations and applications.* Wiley.

Farge, M., Hunt, J. C. R. & Vassilicos, J. C. (eds) 1993 *Wavelets, fractals and Fourier transforms.* Oxford: Clarendon Press.

Gagne, Y. 1987 Etude expérimentale de l'intermittence et des singularités dans le plan complexe en turbulence dévelopée. These de Doctorat, Université de Grenoble, France.

Gagne, Y., Hopfinger, E. J. & Frisch, U. 1988 In *New trends in nonlinear dynamics and pattern phenomena: the geometry of non-equilibrium* (ed. P. Coullet & P. Huene), NATO ASI **237**, 315–319. New York: Plenum.

Hunt, J. C. R., Kevlahan, N., Vassilicos, J. C. & Farge, M. 1993 Wavelets, fractals and Fourier transforms: detection and analysis of structure. In *Wavelets, fractals and Fourier transforms* (ed. M. Farge, J. C. R. Hunt & J. C. Vassilicos). Oxford: Clarendon Press.

Hunt, J. C. R. & Vassilicos, J. C. 1991 Kolmogorov's contributions to the physical and geometrical understanding of small-scale turbulence and recent developments. *Proc. R. Soc. Lond.* A **434**, 183–210.

Jiménez, J., Wray, A. A., Saffman, P. G. & Rogallo, R. S. 1993 The structure of intense vorticity in homogeneous isotropic turbulence. *J. Fluid Mech.* **255**, 65–90.

Jones, J. G., Thomas, R. W. & Earwicker, P. G. 1991 Multiresolution analysis of remotely sensed imagery. *Int. J. Remote Sensing* **12**, 107–124.

Lundgren, T. S. 1993 A small-scale turbulence model. *Phys. Fluids* A**5**, 1472–1483.

Malik, N. A. & Vassilicos, J. C. 1994 Eulerian and Lagrangian scaling properties of randomly advected vortex tubes. *Fluid Mech.* (Submitted.)

Mandelbrot, B. B. 1982 *The fractal geometry of nature.* New York: W.H. Freeman.

Mendès-France, M. 1991 Dimension and entropy of regular curves. In *Fractals: non-integral dimensions and applications* (ed. G. Cherbit). Chichester: Wiley.

Meneveau, C. 1991 Analysis of turbulence in the orthonormal wavelet representation. *J. Fluid Mech.* **232**, 469–520.

Moffatt, H.K. 1993 Spiral structures in turbulent flow. In *Wavelets, fractals and Fourier transforms* (ed. M. Farge, J. C. R. Hunt & J. C. Vassilicos). Oxford: Clarendon Press.

Orey, S. 1970 Gaussian sample functions and the Hausdorff dimension of level crossings. *Z. Wahrscheinlichkeitstheorie verw. Geb.* **15**, 249.

Ottino, J. 1989 *The kinematics of mixing.* Cambridge University Press.

Richardson, L. F. 1922 *Weather prediction by numerical process.* Cambridge University Press.

Sreenivasan, K. R. 1991 Fractals and multifractals in fluid turbulence. *A. Rev. Fluid Mech.* **23**, 539.

Vassilicos, J. C. & Fung, J. C. R. 1994 The self-similar topology of passive interfaces advected by two-dimensional turbulence-like flows. *Phys. Fluids.* (Submitted.)

Vassilicos, J. C. & Hunt, J. C. R. 1991 Fractal dimensions and spectra of interfaces with application to turbulence. *Proc. R. Soc. Lond.* A **435**, 505–534.

Vassilicos, J. C., Moquin, B. P. & Brasseur, J. G. 1993 Self-similar spiral flow structure in low Reynolds number isotropic and decaying turbulence. *J. Fluid Mech.* (Submitted.)

Vermeer, P. L. & Alkemade, J. A. H. 1993 Multiscale segmentation of well logs. In *Wavelets, fractals and Fourier transforms* (ed. M. Farge, J. C. R. Hunt & J. C. Vassilicos). Oxford: Clarendon Press.

Received 29 October 1993; accepted 11 April 1994